Journal of
Mechanical
Science and
Technology

Journal of Mechanical Science and Technology 21 (2007) 1028~1038

Identification of the Types of Rotor Systems Using Directional Frequency Spectrum

Dong-Ju Han*

Korea Institute of Aerospace Technology, 461-1 Jeonmin-dong, Yusung-gu, Daejeon, Korea

(Manuscript Received October 16, 2006; Revised April 2, 2007; Accepted April 3, 2007)

Abstract

Identifying the classification of rotor systems is prerequisite for clear determination of the fault analysis and precise parameter identification for the rotor system, through which operating conditions may be rationally ascertained. For this purpose, the simple creative technique associated with the directional frequency spectrum (dFS) is proposed by using an inherent property of rotor system. Also the features and the dynamic characteristics of the rotor systems relating to the harmonic modes are investigated.

Keywords: Identification; Types; Rotor systems; Directional frequency spectrum; Harmonic solution; Stability

1. Introduction

Predictive identification from condition monitoring of the rotating machinery can greatly reduces the catastrophic failure and unnecessary maintenance so that utilization of the parts can be improved. Much effort has been made to develop the diagnostic methodology of the rotating machinery (Lee, 2000; Iman, 1989; Davis, 1998; Dewell, 1984; Muszynska, 1996). However, most of the efforts have been made on the isotropic rotor system in which the consideration of the operational features due to other types of rotor systems are entirely excluded, thus the cause of the phenomena from the fault may be misunderstood and leads to the wrong decision to repair the fault. Here, among other symptoms to deviate the features of the isotropic rotor systems, several types may exist; an occurrence breathing crack in the sense that it has basically 2X frequency due to the rotor weight (Iman, 1989) but the asymmetric and general rotor systems have the same features due to the rotor weight; a misalignment with an unbalance causes basically 1X and 2X frequencies (Dewell, 1984) but the asymmetric and general rotor systems have the same ones due to the unbalance and rotor weight; sub- or super-harmonics such as aero-elastic or blade tuned vibration effects, ball bearing defects and oil whirl or whip, etc., whose properties are likely to be combined with those by non-isotropic rotor systems. Consequently for rigorous diagnosis of operational conditions the types of the rotor systems with relevant features should be clearly identified in advance to analyze the cause of failures.

According to the non-isotropic properties of the rotor and stator in the rotating machinery, the types of rotor systems can be classified as four as follows (Lee, 1993~2006; Genta, 1988; Irretier, 1999) : *isotropic (symmetric) rotor system*-both the rotor and the stator are axisymmetric; *anisotropic rotor system*-the rotor is axisymmetric but the stator is not, such as the typical fluid-film bearing and the magnetic or hydrostatic bearing with a comparatively heavy rotor weight, which have a anisotropic stiffness and damping properties; *asymmetric rotor system*-the stator is

*Corresponding author. Tel.: +82 41 864 2177, Fax.: +82 41 864 2035
E-mail address: djhan@sunaerosys.com

axisymmetric but the rotor is not, such as the two pole generator with asymmetric moment of rotor inertia, a shaft with keyway or rectangular cross section with asymmetric stiffness, and two shafts in parallel connected by a couple of gears; *general rotor system*- neither the rotor nor the stator is axisymmetric, as a combined case of those three illustrated systems, which is real in industry.

As another aspect of identification of the rotating machinery, modeling a system associated with parameter identification is normally assumed to be performed with an isotropic model (Davis, 1998), irrespective of the types of the rotor systems, thereby the modeling error due to the different type of rotor system may be induced. Thus the identification of the rotor type is prerequisite for more precise model for system identification. Furthermore, for performing the modal analysis of rotor systems, it is imperative to identify the feature of the corresponding rotor type. In this respect, provided that the dynamic characteristics such as the unbalance response, critical speeds and stability according to the rotor types may be significantly altered, knowledge about such properties are essential in gaining an adequate physical understanding of practical rotor systems.

In this paper, using the directional frequency spectrum (dFS) representing the harmonic analysis, which is based on the results of the complex modal analysis (Lee, 1993 ~ 2006), the method to identify the types of rotor systems has been developed by analyzing the characteristics of the harmonic mode, with simple harmonic excitations. The features and the dynamic characteristics according to the rotor types are also investigated by introducing the influence coefficients from the harmonic balance method whose effectiveness is verified by comparing the results with those from the modal analysis, thereby the alternative analysis method identifying the system property and estimating the strength of the harmonics due to the anisotropy and asymmetry is suggested.

2. Harmonic analysis for rotor systems

2.1 Derivation of harmonic response

For a general rotor system with rotating and stationary asymmetry, neglecting the stator (or bearing) mass effect, the equation of motion can be written in the complex stationary coordinates, referring to Fig. 1, as (Lee, 1993~2006; Genta, 1988; Irretier, 1999)

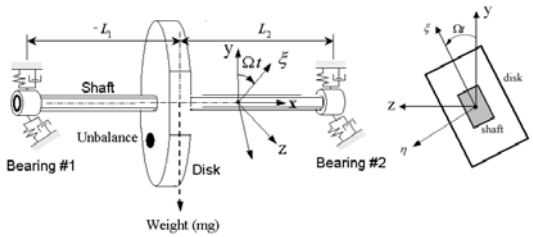

Fig. 1. Simple general rotor model for simulation.

$$\mathbf{M}_f\ddot{\mathbf{p}}(t)+\mathbf{C}_f\dot{\mathbf{p}}(t)+\mathbf{K}_f\mathbf{p}(t)+\left[\mathbf{C}_b\dot{\bar{\mathbf{p}}}(t)+\mathbf{K}_b\bar{\mathbf{p}}(t)\right] +e^{j2\Omega t}\left[\mathbf{M}_r\ddot{\bar{\mathbf{p}}}(t)+\mathbf{C}_r\dot{\bar{\mathbf{p}}}(t)+\mathbf{K}_r\bar{\mathbf{p}}(t)\right]=\mathbf{g}(t). \quad (1)$$

Here, the Nx1 complex response and force vectors, $\mathbf{p}(t)$ and $\mathbf{g}(t)$, defined by the real response vectors, $\mathbf{y}(t)$ and $\mathbf{z}(t)$, and the real input vectors, $\mathbf{f}_y(t)$ and $\mathbf{f}_z(t)$, respectively, are

$$\mathbf{p}(t)=\mathbf{y}(t)+j\mathbf{z}(t),\ \bar{\mathbf{p}}(t)=\mathbf{y}(t)-j\mathbf{z}(t),$$
$$\mathbf{g}(t)=\mathbf{f}_y(t)+j\mathbf{f}_z(t),\ \bar{\mathbf{g}}(t)=\mathbf{f}_y(t)-j\mathbf{f}_z(t), \quad (2)$$

where j means the imaginary number; $\mathbf{g}(t)$ includes the force and moment; Ω is the rotational speed; '-' denotes the complex conjugate henceforth; $\mathbf{M}$, $\mathbf{C}$ and $\mathbf{K}$ are the $N\times N$ complex matrices representing the generalized mass, damping and stiffness, respectively; and the subscripts f, b, and r refer to the symmetric, anisotropic and asymmetric properties, respectively. Detailed properties of the physical parameters are described and illustrated in Appendix A.

For an isotropic rotor system; $\mathbf{C}_b=\mathbf{K}_b=\mathbf{M}_r=\mathbf{C}_r=\mathbf{K}_r=\mathbf{0}$, for an anisotropic rotor system; $\mathbf{M}_r=\mathbf{C}_r=\mathbf{K}_r=\mathbf{0}$; and, for an asymmetric rotor system; $\mathbf{C}_b=\mathbf{K}_b=\mathbf{0}$.

From Eq. (1) and its complex conjugate form, the complex equation of motion can be constructed as

$$\mathbf{M}(t)\ddot{\mathbf{q}}(t)+\mathbf{C}(t)\dot{\mathbf{q}}(t)+\mathbf{K}(t)\mathbf{q}(t)=\mathbf{f}(t), \quad (3)$$

where

$$\mathbf{q}(t)\equiv\begin{Bmatrix}\mathbf{p}(t)\\ \bar{\mathbf{p}}(t)\end{Bmatrix},\ \mathbf{f}(t)\equiv\begin{Bmatrix}\mathbf{g}(t)\\ \bar{\mathbf{g}}(t)\end{Bmatrix},$$
$$\mathbf{M}(t)=\begin{bmatrix}\mathbf{M}_f & \mathbf{M}_r e^{j2\Omega t}\\ \bar{\mathbf{M}}_r e^{-j2\Omega t} & \bar{\mathbf{M}}_f\end{bmatrix},$$
$$\mathbf{C}(t)=\begin{bmatrix}\mathbf{C}_f & \mathbf{C}_b+\mathbf{C}_r e^{j2\Omega t}\\ \bar{\mathbf{C}}_b+\bar{\mathbf{C}}_r e^{-j2\Omega t} & \bar{\mathbf{C}}_f\end{bmatrix},$$

$$\mathbf{K}(\mathrm{t})=\begin{bmatrix}\mathbf{K}_{\mathrm{f}} & \mathbf{K}_{\mathrm{b}}+\mathbf{K}_{\mathrm{r}}e^{j2\Omega t}\\ \bar{\mathbf{K}}_{\mathrm{b}}+\bar{\mathbf{K}}_{\mathrm{r}}e^{-j2\Omega t} & \bar{\mathbf{K}}_{\mathrm{f}}\end{bmatrix}.$$

Equation (3) can be rewritten in the state space form as

$$\mathbf{A}(\mathrm{t})\dot{\mathbf{w}}(\mathrm{t})=\mathbf{B}(\mathrm{t})\mathbf{w}(\mathrm{t})+\mathbf{F}(\mathrm{t}), \tag{4}$$

where

$$\mathbf{A}(\mathrm{t})=\begin{bmatrix}\mathbf{0} & \mathbf{M}(\mathrm{t})\\ \mathbf{M}(\mathrm{t}) & \mathbf{C}(\mathrm{t})\end{bmatrix},\quad \mathbf{B}(\mathrm{t})=\begin{bmatrix}\mathbf{M}(\mathrm{t}) & \mathbf{0}\\ \mathbf{0} & -\mathbf{K}(\mathrm{t})\end{bmatrix},$$
$$\mathbf{w}(\mathrm{t})=\begin{Bmatrix}\dot{\mathbf{q}}(\mathrm{t})\\ \mathbf{q}(\mathrm{t})\end{Bmatrix},\quad \mathbf{F}(\mathrm{t})=\begin{Bmatrix}\mathbf{0}\\ \mathbf{f}(\mathrm{t})\end{Bmatrix}.$$

The detailed procedure using Floquet theory for the modal analysis of this periodically time-varying system in homogeneous part of Eq. (4), which has been developed, are listed in (Lee, 2006; Genta, 1988; Irretier, 1999), therefore the detailed process is not treated here, instead let the main results of the harmonic solution be presented such that for the harmonic input, $\mathbf{g}(t)=\mathbf{g}\,e^{j\omega t}$, where $\mathbf{g}$ is the input vector and ω is the input rotational frequency, the harmonic solution by the harmonic input can be given in the form of (Genta, 1988)

$$\mathbf{p}(\mathrm{t})=\sum_{n=-\infty}^{\infty}\left\{\mathbf{p}_n\cdot e^{\mathrm{j}(\omega+2n\Omega)t}+\tilde{\mathbf{p}}_n\cdot e^{-\mathrm{j}(\omega+2n\Omega)t}\right\}, \tag{5}$$

where the harmonic coefficients, $\mathbf{p}_{\mathrm{n}}$, $\tilde{\mathbf{p}}_{\mathrm{n}}$, reduce the dFS for each harmonic mode from the harmonic analysis.

Thus, the harmonic response of the general rotor system can be given by

$$\begin{aligned}\mathbf{p}(\mathrm{t})\cong{}&\mathbf{p}_{-1}e^{\mathrm{j}(\omega-2\Omega)t}+\tilde{\mathbf{p}}_{-1}e^{-\mathrm{j}(\omega-2\Omega)t}+\mathbf{p}_0e^{\mathrm{j}\omega t}\\&+\tilde{\mathbf{p}}_0e^{-\mathrm{j}\omega t}+\mathbf{p}_1e^{\mathrm{j}(\omega+2\Omega)t}+\tilde{\mathbf{p}}_1e^{-\mathrm{j}(\omega+2\Omega)t},\end{aligned} \tag{6}$$

The coefficients, $\mathbf{p}_n$, $\tilde{\mathbf{p}}_n$, can be obtained by the modal parameters from the complete modal analysis given in references (Lee, 2006; Irretier, 1999), however, the rigorous modal analysis is rather inefficient in that the focus is rested only on the patterns of dSs represented by the influence coefficients, which are required to interpret the corresponding harmonic modes. The harmonic balance method (Genta, 1988) can be effectively utilized to this purpose, which is readily available to derive algebraically as; the direct substitution of the coefficients, $\mathbf{p}_n$ and $\tilde{\mathbf{p}}_n$ in Eq. (5), into the equation of motion (1) reduces to the form of

$$\begin{aligned}\sum_{n=-\infty}^{\infty}\Big[&(\mathbf{D}_{\mathrm{f};-n}\mathbf{p}_n+\mathbf{D}_{\mathrm{b};-n}\bar{\tilde{\mathbf{p}}}_n)e^{\mathrm{j}(2n\Omega+\omega)t}\\&+(\mathbf{D}_{\mathrm{f};n}\tilde{\mathbf{p}}_n+\mathbf{D}_{\mathrm{b};n}\bar{\mathbf{p}}_n)e^{-\mathrm{j}(2n\Omega+\omega)t}\\&+(\mathbf{D}_{\mathrm{r};-n}\bar{\tilde{\mathbf{p}}}_ne^{\mathrm{j}(2n\Omega+\omega)t}\\&+\mathbf{D}_{\mathrm{r;k}}\bar{\mathbf{p}}_ne^{-\mathrm{j}(2n\Omega+\omega)t})e^{\mathrm{j}2\Omega t}\Big]=\mathbf{g}(\mathrm{t}).\end{aligned} \tag{7}$$

The general harmonic inputs can be expressed in the form of $\mathbf{g}(\mathrm{t})=\sum_{n=-\infty}^{\infty}\left\{\mathbf{g}_n\cdot e^{\mathrm{j}(\omega+2n\Omega)t}+\tilde{\mathbf{g}}_n\cdot e^{-\mathrm{j}(\omega+2n\Omega)t}\right\}$, where $\mathbf{g}_n$ and $\tilde{\mathbf{g}}_n$ are the vectors with magnitudes and phases of the n-th harmonic inputs. Then equating the coefficients of exponential terms in Eq. (7) to zero yields the set of algebraic equations as

$$\begin{aligned}&\mathbf{D}_{\mathrm{b};-n}\bar{\tilde{\mathbf{p}}}_n+\mathbf{D}_{\mathrm{f};-n}\mathbf{p}_n+\mathbf{D}_{\mathrm{r};-n}\bar{\tilde{\mathbf{p}}}_{n-1}=\mathbf{g}_{\mathrm{n}},\\&\bar{\mathbf{D}}_{\mathrm{r};n}\mathbf{p}_{n+1}+\bar{\mathbf{D}}_{\mathrm{f};n}\bar{\tilde{\mathbf{p}}}_n+\bar{\mathbf{D}}_{\mathrm{b};n}\mathbf{p}_n=\tilde{\bar{\mathbf{g}}}_n,\end{aligned} \tag{8}$$

where the dynamic stiffnesses are

$$\begin{aligned}&\mathbf{D}_{\mathrm{i};n}(\omega)=-(2n\Omega-\omega)^2\mathbf{M}_{\mathrm{i}}-\mathrm{j}(2n\Omega-\omega)\mathbf{C}_{\mathrm{i}}+\mathbf{K}_{\mathrm{i}},\\&\mathrm{i=f,b,r},\quad n=0,\pm1,\pm2,.....\end{aligned}$$

Here ω is omitted in $\mathbf{D}_{\mathrm{i};n}(\omega)$ for notational simplicity henceforth.

For $\mathbf{g}(\mathrm{t})=\mathbf{g}\cdot e^{j\omega t}$, $\mathbf{g}(\mathrm{t})$ is designated by: the forward and backward unbalances are the case where $\omega=\Omega$, and $\omega=-\Omega$, respectively, and the weight is the case where $\omega=0$, etc., the new forms of $\mathbf{p}_n$ and $\tilde{\mathbf{p}}_n$ can then be obtained from reducing Eq. (8) to the matrix algebraic equations in Hill's form, for every n, as

$$\begin{Bmatrix}\vdots\\ \bar{\tilde{\mathbf{p}}}_1\\ \mathbf{p}_1\\ \bar{\tilde{\mathbf{p}}}_0\\ \mathbf{p}_0\\ \bar{\tilde{\mathbf{p}}}_{-1}\\ \mathbf{p}_{-1}\\ \vdots\end{Bmatrix}=\begin{bmatrix}\ddots & & & & & \iddots\\ & \bar{\mathbf{D}}_{\mathrm{f};1} & \bar{\mathbf{D}}_{\mathrm{b};1} & & & \\ & \mathbf{D}_{\mathrm{b};-1} & \mathbf{D}_{\mathrm{f};-1} & \mathbf{D}_{\mathrm{r};0} & \mathbf{0} & \\ & & \bar{\mathbf{D}}_{\mathrm{r};1} & \bar{\mathbf{D}}_{\mathrm{f};0} & \bar{\mathbf{D}}_{\mathrm{b};0} & \\ & & & \mathbf{D}_{\mathrm{b};0} & \mathbf{D}_{\mathrm{f};0} & \mathbf{D}_{\mathrm{r};1}\\ & & \mathbf{0} & & \bar{\mathbf{D}}_{\mathrm{r};0} & \bar{\mathbf{D}}_{\mathrm{f};-1} & \bar{\mathbf{D}}_{\mathrm{b};-1}\\ & & & & & \mathbf{D}_{\mathrm{b};1} & \mathbf{D}_{\mathrm{f};1}\\ \iddots & & & & & & \ddots\end{bmatrix}^{-1}\begin{Bmatrix}\vdots\\ \mathbf{0}\\ \mathbf{0}\\ \mathbf{0}\\ \mathbf{g}\\ \mathbf{0}\\ \mathbf{0}\\ \mathbf{0}\\ \vdots\end{Bmatrix}=\begin{bmatrix}\vdots\\ \mathbf{H}_{\mathbf{g}_0\bar{\mathbf{p}}_1}\\ \mathbf{H}_{\mathbf{g}_0\mathbf{p}_1}\\ \mathbf{H}_{\mathbf{g}_0\bar{\mathbf{p}}_0}\\ \mathbf{H}_{\mathbf{g}_0\mathbf{p}_0}\\ \mathbf{H}_{\mathbf{g}_0\bar{\mathbf{p}}_{-1}}\\ \mathbf{H}_{\mathbf{g}_0\mathbf{p}_{-1}}\\ \vdots\end{bmatrix}\mathbf{g}, \tag{9}$$

which results in the Hill's infinite determinants with 3N bandwidths, where the matrices, $\mathbf{D}_{\mathrm{f;m}}$, $\mathbf{D}_{\mathrm{b;m}}$ and $\mathbf{D}_{\mathrm{r;m}}$, are related to the isotropy, anisotropy and

asymmetry of a general rotor system, respectively. Here the framed parts denoted by solid, dotted and dot solid areas denote the isotropic, anisotropic and asymmetric rotor systems, respectively (Lee, 1993~ 2006; Genta, 1988), henceforth, as the limiting cases of the general rotor system. The elements comprised in the inverse matrix of the dynamic stiffness matrix reduce to the influence coefficient matrix, **H**, which is described in Appendix B. The influence coefficients derived here are numerically identical to the so-called directional frequency response functions (dFRFs) representing the previous modal analysis (Lee, 1993~ 2006). Thus, likewise in the modal analysis, we can find that the influence coefficients can be utilized as the indicator for the presence of the anisotropy and/or the asymmetry in a similar way to the dFRFs. The crucial difference of the two methods is that the influence coefficients presented here are achieved from the single-input/multiple-outputs relation described by the direct physical parameters whereas the dFRFs from the modal analysis are achieved from the multiple-inputs/ single-output relation described by the modal parameters.

From Eq. (9), the coefficients of the harmonic response can then be given in the form of

$$\begin{aligned}
&\mathbf{p}_{-1}=\mathbf{H}_{\mathbf{g};0\mathbf{p};-1}(\omega)\mathbf{g}, \quad \tilde{\mathbf{p}}_{-1}=\overline{\mathbf{H}}_{\mathbf{g};0\hat{\mathbf{p}};-1}(\omega)\overline{\mathbf{g}},\\
&\mathbf{p}_{0}=\mathbf{H}_{\mathbf{g};0\,\mathbf{p};0}(\omega)\mathbf{g}, \quad \tilde{\mathbf{p}}_{0}=\overline{\mathbf{H}}_{\mathbf{g};0\,\hat{\mathbf{p}};0}(\omega)\overline{\mathbf{g}},\\
&\mathbf{p}_{1}=\mathbf{H}_{\mathbf{g};0\mathbf{p};1}(\omega)\mathbf{g}, \quad \tilde{\mathbf{p}}_{1}=\overline{\mathbf{H}}_{\mathbf{g};0\hat{\mathbf{p}};1}(\omega)\overline{\mathbf{g}}.
\end{aligned} \tag{10}$$

Note that as a limiting case of the general rotor system, the isotropic, anisotropic and asymmetric systems can be expressed by the closed form solutions with the harmonic coefficients, $\mathbf{p}_0$, $\mathbf{p}_0$ and $\tilde{\mathbf{p}}_0$, $\mathbf{p}_0$ and $\tilde{\mathbf{p}}_{-1}$, respectively, such that the harmonic response for the asymmetric rotor system becomes

$$\mathbf{p}(\mathrm{t})=\tilde{\mathbf{p}}_{-1}e^{-\mathrm{j}(\omega-2\Omega)t}+\mathbf{p}_0e^{\mathrm{j}\omega t}, \tag{11}$$

likewise, for the anisotropic rotor system, the harmonic response is

$$\mathbf{p}(\mathrm{t})=\mathbf{p}_0e^{\mathrm{j}\omega t}+\tilde{\mathbf{p}}_0e^{-\mathrm{j}\omega t}, \tag{12}$$

and, for the isotropic rotor system, the harmonic response is

$$\mathbf{p}(\mathrm{t})=\mathbf{p}_0e^{\mathrm{j}\omega t}, \tag{13}$$

In this case the eigenvalues can be obtained from the latent value problem associated with the $\lambda-matrix$ of degree 2, $\mathbf{D}_2(\lambda)$, (Lee, 1993; Lancaster, 1985) for a reduced Hill's matrix of 6N order, can be given by

$$\begin{aligned}
\mathbf{D}_2(\lambda)&=\begin{vmatrix}
\bar{\mathbf{D}}_{\mathrm{f};1}(\lambda) & \bar{\mathbf{D}}_{\mathrm{b};1}(\lambda) & & & & \\
\mathbf{D}_{\mathrm{b};-1}(\lambda) & \mathbf{D}_{\mathrm{f};-1}(\lambda) & \mathbf{D}_{\mathrm{r};0}(\lambda) & & \mathbf{0} & \\
 & \bar{\mathbf{D}}_{\mathrm{r};1}(\lambda) & \bar{\mathbf{D}}_{\mathrm{f};0}(\lambda) & \bar{\mathbf{D}}_{\mathrm{b};0}(\lambda) & & \\
 & & \mathbf{D}_{\mathrm{b};0}(\lambda) & \mathbf{D}_{\mathrm{f};0}(\lambda) & \mathbf{D}_{\mathrm{r};1}(\lambda) & \\
 & \mathbf{0} & & \bar{\mathbf{D}}_{\mathrm{r};0}(\lambda) & \bar{\mathbf{D}}_{\mathrm{f};-1}(\lambda) & \bar{\mathbf{D}}_{\mathrm{b};-1}(\lambda)\\
 & & & & \mathbf{D}_{\mathrm{b};1}(\lambda) & \mathbf{D}_{\mathrm{f};1}(\lambda)
\end{vmatrix}\\
&=\lambda^2\boldsymbol{E}_2+\lambda\boldsymbol{E}_1+\boldsymbol{E}_0=\mathbf{0},
\end{aligned} \tag{14}$$

where the form of $\lambda=j\omega$ is taken for the latent value problem in Eq. (9), and $\boldsymbol{E}_2$, $\boldsymbol{E}_1$, $\boldsymbol{E}_0$, are the coefficients of the $\lambda-matrix$. The stability of rotor systems (Lee, 2005; 2006; Meng, 2000) can be found from real parts of system eigenvalues or visually can be seen in the whirl charts by discontinuous regions of line groups particularly for rotor system with dissimilar shaft stiffnesses such as an asymmetric and general rotor systems which will be seen in simulated results.

3. Classification of rotor systems by harmonic patterns

3.1 Detection of dFS from the signal

The dFS made from the measured signal gives the information on the harmonic modes, i.e. mX (m= $\pm1,\pm2,\pm3,\ldots$) spectra. The modes transformed by finite discrete Fourier transform (DFT), $\mathbf{P}(\mathrm{k})$, of the signal $\mathbf{p}(\mathrm{t})$ consist of m harmonics such as, $\mathbf{p}(\mathrm{t})=\sum\mathbf{p}_\mathrm{m}\mathrm{e}^{j\omega_\mathrm{m}\mathrm{t}}$, with the harmonic frequency $\omega_\mathrm{m}=\mathrm{m}\varpi_0=2\pi\mathrm{m/T}$, where ω_0 is the rotational frequency. It can be written as (Lee, 2000; Bendat, 1986)

$$\begin{aligned}
\mathbf{P}(\mathrm{k})&=\Delta\mathrm{t}\sum_{\mathrm{n}=0}^{\mathrm{N}-1}\mathbf{p}(\mathrm{n}\Delta\mathrm{t})\,\mathrm{e}^{-\mathrm{j}\,\omega_\mathrm{k}\,\mathrm{n}\,\Delta\mathrm{t}}\\
&=\Delta\mathrm{t}\sum_{\mathrm{n}=0}^{\mathrm{N}-1}\sum_{\mathrm{m}}\mathbf{p}_\mathrm{m}\mathrm{e}^{-\mathrm{j}\,(\omega_\mathrm{k}-\omega_\mathrm{m})\,\mathrm{n}\,\Delta\mathrm{t}}\\
&=\sum_{\mathrm{m}}\mathbf{p}_\mathrm{m}\left(\Delta\mathrm{t}\sum_{\mathrm{n}=0}^{\mathrm{N}-1}\mathrm{e}^{-\mathrm{j}\,2\pi(\mathrm{k}-\mathrm{m})\frac{\mathrm{n}}{\mathrm{N}}}\right),
\end{aligned} \tag{15}$$

where

$$\omega_\mathrm{k}=\frac{2\pi\mathrm{k}}{\mathrm{T}}=\frac{2\pi\mathrm{k}}{\mathrm{N}\Delta\mathrm{t}}=\mathrm{k}\Delta\omega,\ \mathrm{k}=-\frac{\mathrm{N}}{2}+1,\ -\frac{\mathrm{N}}{2}+2,\ \ldots,\ \frac{\mathrm{N}}{2}-1,\ \frac{\mathrm{N}}{2},$$

and Δt is the sampling interval, N is the even number of samples, Δω is the frequency resolution which becomes the rotational frequency. Here $\mathbf{p}$ (t) with the harmonic coefficient $\mathbf{p}_m$ behaves over the frequency resolution bandwidth Δω=2π/T which appears a dS at the m-th harmonic, mX. In general the ideal harmonic signal without noise effect can be transformed to near the finite impulse DFT value by choosing the appropriate sampling interval and number of samples to satisfy the periodicity. Analytically the harmonic pattern of $\mathbf{p}$ (t) shows the finite impulse value such that $\mathbf{P}(\omega)=\sum_m \mathbf{p}_m \delta(\omega-\omega_m)$, however, in practice, the leakage problem occurs in truncated data that is not matched with period T. To avoid this problem the resolution bandwidth, $\Delta\omega$ should be designed sufficiently lower than the harmonic frequency, ω_m, in addition to windowing the truncated data (Bendat, 1986).

3.2 Harmonic patterns of rotor systems by simple harmonic excitations

The key advantage of dFS for rotor systems is that the harmonic components with directivity can be directly acquired from Fourier transform of the complex-valued signal representing planar whirl motion derived in Eq. (5). The positive (negative) frequency components appearing in dFS physically correspond to forward (backward) whirling components. Thus, by analyzing the feature of the dFS via various harmonic inputs the detection method of the rotor types or further diagnosis method for any constructive defect could be effectively created.

For example of rotor systems excited by an unbalance, such harmonics patterns as $\pm(2n+1)$X, $n=1,2,3,...$ in dFS are acquired from Fourier transform of the motion derived in Eq. (6) and Eqs. (11) ~ (13). In general, for an unbalance, isotropic and asymmetric rotors appear only 1X harmonic, anisotropic rotor appears 1X and –1X harmonics, and general rotor appears 1X, –1X, 3X, –3X, and other higher harmonics. We can predict from these results that the unbalance response comprising the forward and/or backward whirling components indicates a circle for isotropic and asymmetric rotors, whereas an ellipse for anisotropic rotor, and Limacon (Lee, 1993) including an ellipse for general rotor system.

Here, let the three combinations of the simple harmonic excitations be considered such as an unbalance, a static load and a backward unbalance excitation. In this paper, assuming that the rotor with relatively heavy weight is located to incur the shaft deflection, let the static load be utilized by a rotor gravity effect, i.e., a rotor weight rather than the further device for static load such as the magnetic exciter. Then, from Eq. (6) and Eqs. (11) ~ (13), the directional frequency spectra (dFSs) according to the excitations are featured as follows:

For an unbalance ($\omega=\Omega$, $\mathbf{g}=\mathbf{g}_u$, $\tilde{\mathbf{g}}=0$), isotropic rotor; 1X ($\mathbf{p}_0$), anisotropic rotor; 1X ($\mathbf{p}_0$) and –1X ($\tilde{\mathbf{p}}_0$), asymmtric rotor; 1X ($\mathbf{p}_0, \tilde{\mathbf{p}}_{-1}$), and general rotor; 1X ($\mathbf{p}_0$, $\tilde{\mathbf{p}}_{-1}$), –1X ($\tilde{\mathbf{p}}_0$), 3X ($\mathbf{p}_1$) and –3X ($\tilde{\mathbf{p}}_1$) or other higher harmonics $\pm 3n$X. For a weight ($\omega=0$, $\mathbf{g}=\mathbf{g}_0$, $\tilde{\mathbf{g}}=0$), isotropic rotor; 0X ($\mathbf{p}_0$), anisotropic rotor; 0X ($\mathbf{p}_0$, $\tilde{\mathbf{p}}_0$), asymmtric rotor; 0X ($\mathbf{p}_0$) and 2X ($\tilde{\mathbf{p}}_{-1}$), and general rotor; 0X ($\mathbf{p}_0$, $\tilde{\mathbf{p}}_0$), 2X ($\mathbf{p}_1$, $\tilde{\mathbf{p}}_{-1}$) and –2X ($\mathbf{p}_{-1}$). For an unbalance plus a weight ($\omega=\Omega$, $\mathbf{g}=\mathbf{g}_u, \mathbf{g}_0$, $\tilde{\mathbf{g}}=0$), isotropic rotor; 1X and 0X ($\mathbf{p}_0$), anisotropic rotor; 1X, –1X and 0X ($\mathbf{p}_0$, $\tilde{\mathbf{p}}_0$), asymmtric rotor; 0X ($\mathbf{p}_0$), 1X ($\mathbf{p}_0, \tilde{\mathbf{p}}_{-1}$) and 2X ($\tilde{\mathbf{p}}_{-1}$), and general rotor; 0X ($\mathbf{p}_0$, $\tilde{\mathbf{p}}_0$), 1X ($\mathbf{p}_0$, $\tilde{\mathbf{p}}_{-1}$), –1X ($\tilde{\mathbf{p}}_0$), 2X ($\mathbf{p}_1$, $\tilde{\mathbf{p}}_{-1}$), –2X ($\mathbf{p}_{-1}$), 3X ($\mathbf{p}_1$) and –3X ($\tilde{\mathbf{p}}_1$). For a backward unbalance excitation ($\omega=\Omega$, $\mathbf{g}=\mathbf{0}$, $\tilde{\mathbf{g}}=\mathbf{g}_{-u}$), isotropic rotor; –1X ($\tilde{\mathbf{p}}_0$), anisotropic rotor; 1X ($\mathbf{p}_0$) and –1X ($\tilde{\mathbf{p}}_0$), asymmtric rotor; –1X ($\tilde{\mathbf{p}}_0$) and 3X ($\mathbf{p}_1$), and general rotor; 1X ($\mathbf{p}_0$, $\tilde{\mathbf{p}}_{-1}$), –1X ($\tilde{\mathbf{p}}_0$), 3X ($\mathbf{p}_1$) and –3X ($\tilde{\mathbf{p}}_1$).

Table 3 summarizes the results of dFSs by other various harmonic inputs applied to the rotor systems. Some notes are induced from the dFSs described in Table 3 that for an unbalance, isotropic and asymmetric rotors are not classified, for a static load (or disk weight), isotropic and anisotropic rotors are not classified, whereas a backward unbalance can classify the four rotor types definitely. As a rule we can suggest that the simple and effective methods to identify the types of rotor system are an unbalance plus disk weight and a backward unbalance excitation. Ideally, if and only if an inherent unbalance in rotor system can be completely cancelled and the weight effect is neglected, a backward unbalance excitation is more clear and definite identifier rather than an unbalance associated with a rotor weight. However, if the rotor weight is considerably heavy and an unbalance exists in some degree, only the sensors are necessary to identify the rotor systems without an exciter, which is preferred to the most efficient method in practice.

4. Numerical simulation

In this simulation, a simple, yet general rotor system model, which consists of a rigid rotor with asymmetric mass moments of inertia, a massless shaft with asymmetric shaft stiffnesses, and two orthotropic bearings, is introduced in Fig. 1. For the types of rotor systems described in Table 1, the physical data used in the proposed model are listed in Table 2.

Figure 2 shows the whirl speeds of the rotor systems. The unstable regions, due to the presence of rotating asymmetry (Lee, 2005; 2006; Meng, 2000),

Table 1. Classification of rotor systems.

Property \ Rotor type	Isotropic rotor	Anisotropic rotor	Asymmetric rotor	General rotor
Asymmetry	0	0	δ	δ
Anisotropy	0	Δ	0	Δ

Table 2. Physical properties of the simple general rotor model.

Location	Property
Disk	$\rho = 7{,}850$ kg.m^{-3}, $D = 400$ mm, $l_D = 30$ mm, $M = \rho\pi l_D D^2/4 = 29.6$ kg $J_p = \rho M D^2/8 = 0.5918$ kg.m^2, $J = \rho M\left(3D^2/4 + l_D^2\right)/12 = 0.298$ kg.m^2 $\Delta J = \delta J$, δ (degree of asymmetry) = 0.3 unbalance ; $\mathbf{U}_0 = \text{me}\,e^{j\beta} = 0.0001M \times 0.75\text{D}\,e^{j30^\circ}$ $= 76.9 + j44.4$ g.cm
Shaft	$E = 2.07\times10^{11}$ N.m^{-2}, $L_1 = 0.2$ m, $L_2 = 0.3$ m, $d = 40$ mm $I = \pi d^4/64$, $\Delta I = \delta I$, $k_r = 1.1\times10^7$ N.m^{-1}, $k_\theta = 5.85\times10^5$ N.rad^{-1} $k_{r\theta} = -1.46\times10^6$ N.rad^{-1}.m^{-1}, $\Delta k_{rr} = \delta k_{rr}$, $\Delta k_\theta = \delta k_\theta$, $\Delta k_{r\theta} = \delta k_{r\theta}$ $c_r = 50$ Ns.m^{-1}, $c_\theta = 30$ Ns.rad^{-1}, $\delta = 0.3$
Bearings	$k_{b1} = k_{b2} = k_b = 5\times10^6$ N.m^{-1}, $\Delta k_{b1} = \Delta k_{b2} = \Delta k_b$, $c_{b1} = c_{b2} = 3{,}000$ Ns.m^{-1} $\Delta c_{b1} = \Delta c_{b2} = 0$, Δ (degree of anisotropy) = 0.3

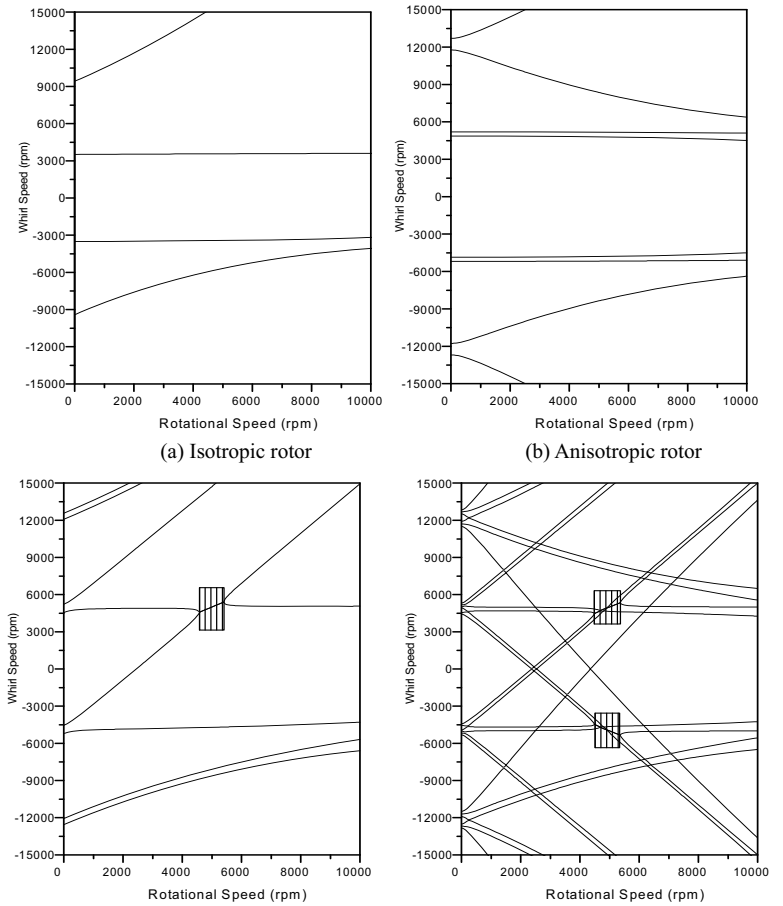

(a) Isotropic rotor (b) Anisotropic rotor

(c) Asymmetric rotor (d) General rotor (Hill's matrix of order 6 N)

(Unstable regions are shaded)

Fig. 2. Whirl charts of rotor systems.

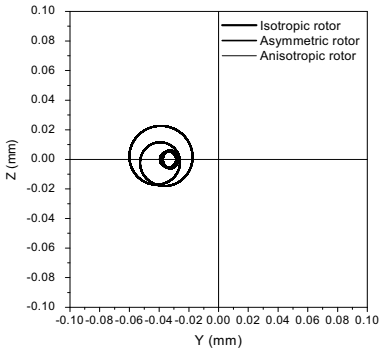

- @ 2000 rpm -

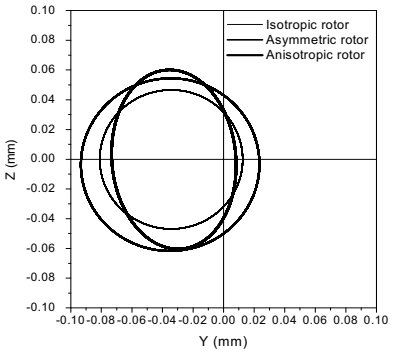

- @ 4000 rpm -

(a) Three types of rotor systems

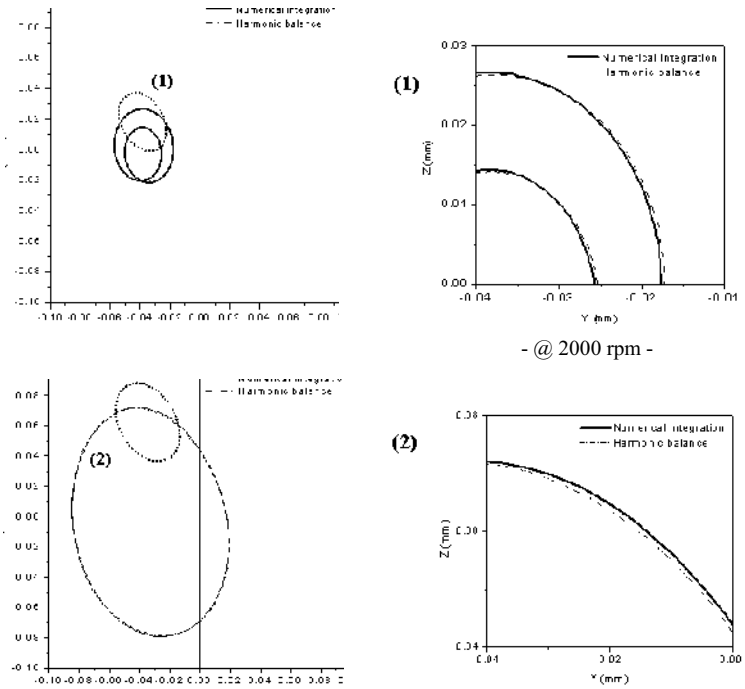

- @ 2000 rpm -

- @ 4000 rpm -

(b) General rotor (Hill's matrix of order 6 N): (1), (2); magnified views

Fig. 3. Whirl orbits by an unbalance and a disk weight.

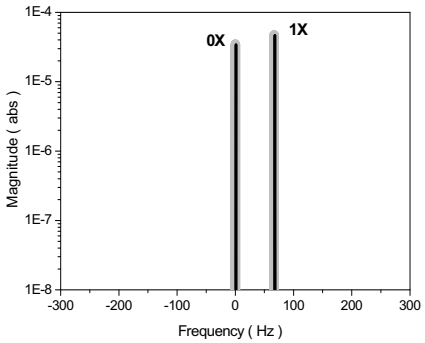

(a) Isotropic rotor

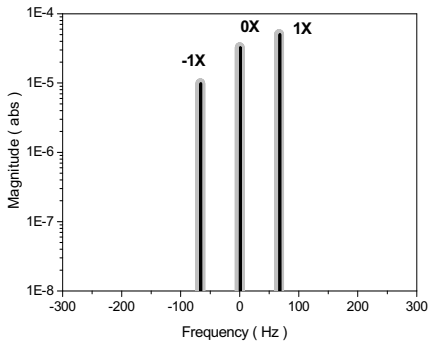

(b) Anisotropic rotor

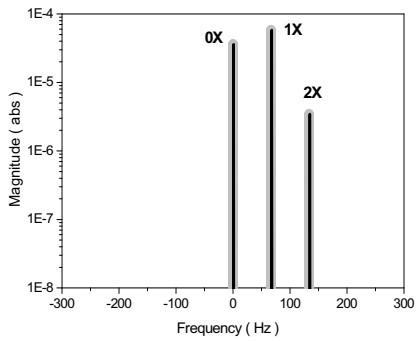

(c) Asymmetric rotor

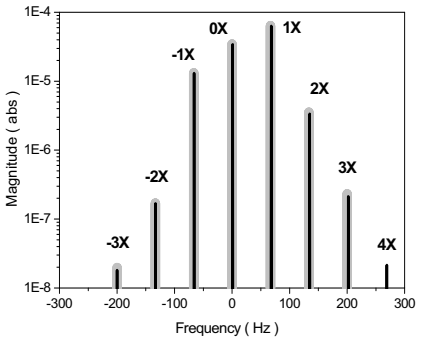

(d) General rotor

(Hill's matrix of order 6N)

Fig. 4. Directional frequency spectra (m) by an unbalance and a disk weight @ 4,000 rpm; harmonic solution, numerical solution.

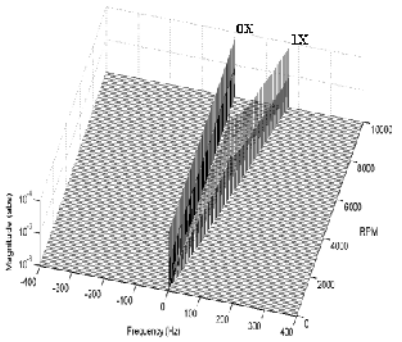

(a) Isotropic rotor

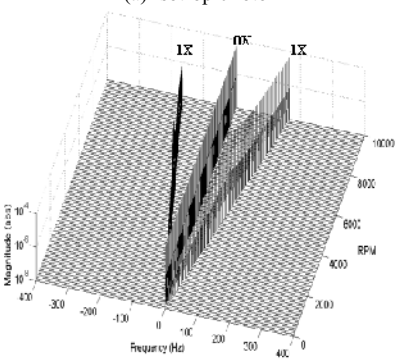

(b) Anisotropic rotor

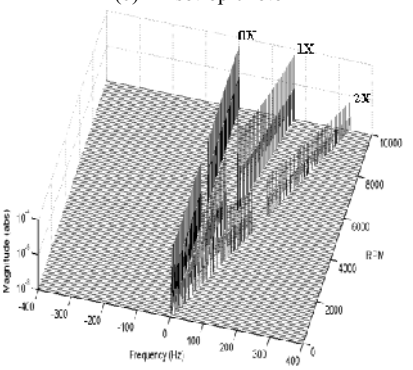

(c) Asymmetric rotor

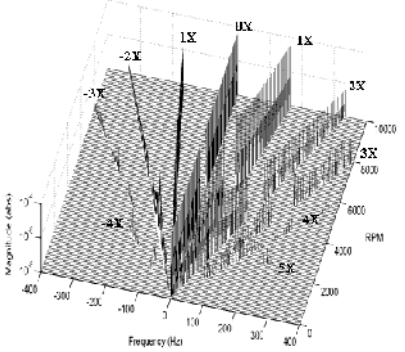

(d) General rotor

Fig. 5. Directional frequency spectra (m) by an unbalance and a disk weight.

can be seen in asymmetric and general rotor systems [marked by hatched region in Figs. 2(c) and (d)].

Figure 3 indicates the whirl orbits of the rotor systems. Figure 3(a) represents solely the results from the harmonic balance method in that any method produces the exact solutions in those three rotor types. On the other hand, considering that for a general rotor system, the solutions from the methods are approximate not like the three rotor types, Fig. 3(b) compares the exact numerical solution with those from the methods by the modal analysis and the harmonic balance. The result from the rigorous modal analysis is slightly more accurate than that from the harmonic balance method. In any case both methods also prove the effectiveness by showing fairly good agreements to the exact numerical solution. Here the shapes are changed from Limacon patterns around low (2,000) rpm to circle and ellipse around high (4,000) rpm, in asymmetric and general rotor systems, respectively, with the fundamental shape of ellipse due to the intrinsic presence of the anisotropy in rotor systems.

Figure 4 compares the numerical solution of dFSs by an unbalance and a weight with those from the influence coefficients which are approximate solution with a finite order of Hill's matrix in general rotor system whereas those are exact in the other types of rotor systems. Figure 5 represents the waterfall plots of dFSs over the rotational speed range of 100-rpm intervals, which is numerically obtained by DFT from the simulated responses. In any case, the magnitude of 0X reflects the static deflection by the disk weight in rotor systems, which is constant irrespectively of the rotational speed. In Figs. 4 and 5, for numerical solution by DFT, the sampling interval and the number of samples are taken by 10,000 Hz and 12, 000 points, respectively, for matching periodicity of the rotational speed. In Fig. 5(c) and (d), the invalid regions are observed in those of the instabilities because of singularity in numerical solution process. In Fig. 4, those from the harmonic balance method show fairly good agreements to the numerical solutions, consequently the effectiveness of the method is reconfirmed. We can see from Figs. 4 and 5 that the unbalance plus weight clearly classify the harmonic patterns of each rotor system as suggested in Table 3, leading to an effective condition to tell the types of rotor systems.

5. Conclusions

The harmonic analysis for identification of the rotor types has been performed. By analyzing the harmonic patterns of directional frequency spectra of the rotor systems, the simple harmonic excitation method to identify the types of rotor systems is proposed by utilizing the unbalance and rotor weight, which is natural and inherent condition without further excitation device. The features and the dynamic characteristics according to the rotor types are investigated by the harmonic balance method whose effectiveness is verified by comparing with the numerical solution.

References

Bendat, J. S., Piersol, A. G., 1986, *Random Data: Analysis and Measurement Procedures*, John Wiley.

Davis, S. S., 1998, "Vibration Analysis of Rotating Machinery Using the Spectral Distribution Function," *Journal of Sound and Vibration,* Vol. 214, No.5, pp. 805~815.

Dewell, D. L. and Mitchell, L. D. 1984, "Detection of a Misaligned Disk Coupling Using Spectrum Analysis," *Journal of Vibration, Acoustics, Stress, and Reliability in Design*, Vol. 106, pp. 9~16.

Genta, B., 1988, "Whirling of Unsymmetrical Rotors: A Finite Element Approach Based on Complex Co-ordinates," *Journal of Sound and Vibration,* Vol. 124, No.1, pp. 27~53.

Iman, I., Azzaro, S. H. and Bankert, R. J., 1989, "Development of an On-Line Rotor Crack Detecting and Monitoring System," *Journal of Vibration, Acoustics, Stress, and Reliability in Design*, Vol. 111, pp. 241~250.

Irretier, H., 1999, "Mathematical Foundations of Experimental Modal Analysis in Rotor Dynamics," *Mechanical Systems and Signal Processing,* Vol. 13, No. 2, pp. 183~191.

Kramer, E., 1993, *Dynamics of Rotors and Foundations*, Springer-Verlag.

Kwon, K. S. and Lee, C. W., 2000, "Random Excitation for Modal Testing of Rotating Machinery: Use of Modulation Technique," *Journal of Sound and Vibration*, Vol. 234, pp. 297~309.

Lancaster, P. and Tismenetsky, M., 1985, *The Theory of Matrices with Application*, Academic Press, Second Edition.

Lee, C. W., 1993, *Vibration Analysis of Rotors*, Kluwer Academic Publishers.

Lee, C. W., Han, D. J. and Hong, S. W., 2006, "Modal Analysis of Periodically Time-varying Linear Rotor Systems Using Floque Theory," 7th IFToMM-Conference on Rotor Dynamics, Vienna, Austra.

Lee, C. W., Han, D. J., Suh, J. H. and Hong, S.W., 2006, "Modal Analysis of Periodically Time-varying Linear Rotor Systems," to Appear in *Journal of Sound and Vibration*.

Meng, G. and Garsh W., 2000, "Stability and Stability Degree of a Cracked Flexible Rotor Supported on Journal Bearing," *Journal of Vibration and Acoustics,* Vol. 122, pp. 116~125.

Muszynska, A., 1996, "Modal Testing of Rotor/ Bearing Systems," *International J. of Analytical and Experimental Modal Analysis*, Vol.1, pp. 15~34.

Ota, H. and Mizutani, K., 1978, "Influence of Unequal Pedestal Stiffness on the stability Regions of a Rotating Asymmetric Shaft," *Journal of Applied Mechanics,* Vol. 45, pp. 400~408.

Suh, J. H., Hong, S. W. and Lee, C. W., 2005, "Modal Aanalysis of Asymmetric Rotor System with Isotropic Stator Using Modulated Coordinates," *Journal of Sound and Vibration*, Vol. 284, pp.651~671.

Appendix A Simple general rotor system for simulation

Consider the general rotor system, consisting of an asymmetric rotor with a rigid disk and two supporting bearings at ends of the massless shaft (Lee, 2006; Ota, 1978), as shown in Fig. 1. The orthotropic bearing stiffness and damping coefficients are assumed to be independent of the rotational speed. For analytical simplicity, the rotating (body-fixed) coordinates $\xi-\eta$ are assumed to be aligned with the principal mass moment of inertia axes of the disk and the principal shaft bending stiffness directions. Then, the equation of motion for the general rotor model reduces to Eq. (1) with the system matrices given by

$$\mathbf{p}=[p_1,p_2,p_3,p_4]^T =[y_d+jz_d,\ \theta_y+j\theta_z,\ y_1+jz_1,\ y_2+jz_2]^T,$$

$$\mathbf{g}=[g_1,g_2,g_3,g_4]^T=[f_{y_d}+jf_{z_d},\ f_{\theta y}+jf_{\theta z},\ 0,\ 0]^T,$$

$$\mathbf{M_f}=\begin{bmatrix} m & 0 & 0 & 0\\ 0 & J & 0 & 0\\ 0 & 0 & 0 & 0\\ 0 & 0 & 0 & 0\end{bmatrix},\quad \mathbf{M_r}=\begin{bmatrix} 0 & 0 & 0 & 0\\ 0 & \Delta J & 0 & 0\\ 0 & 0 & 0 & 0\\ 0 & 0 & 0 & 0\end{bmatrix},$$

$$\mathbf{G}^d=\begin{bmatrix} 0 & 0 & 0 & 0\\ 0 & J_p & 0 & 0\\ 0 & 0 & 0 & 0\\ 0 & 0 & 0 & 0\end{bmatrix},\quad \mathbf{C_b}=\begin{bmatrix} 0 & 0 & 0 & 0\\ 0 & 0 & 0 & 0\\ 0 & 0 & \Delta c_{b1} & 0\\ 0 & 0 & 0 & \Delta c_{b2}\end{bmatrix},$$

$$\mathbf{K_b}=\begin{bmatrix} 0 & 0 & 0 & 0\\ 0 & 0 & 0 & 0\\ 0 & 0 & \Delta k_{b1} & 0\\ 0 & 0 & 0 & \Delta k_{b2}\end{bmatrix}$$

$$\mathbf{C_f^d}=\begin{bmatrix} c_r & 0 & -l_2c_r & -l_1c_r\\ 0 & c_\theta & -jc_\theta/L & jc_\theta/L\\ -l_2c_r & jc_\theta/L & l_2^2c_r-c_\theta/L^2 & l_1l_2c_r-c_\theta/L^2\\ -l_1c_r & -jc_\theta/L & l_1l_2c_r-c_\theta/L^2 & l_1^2c_r-c_\theta/L^2\end{bmatrix},$$

$$\mathbf{C_f^b}=\begin{bmatrix} 0 & 0 & 0 & 0\\ 0 & 0 & 0 & 0\\ 0 & 0 & c_{b1} & 0\\ 0 & 0 & 0 & c_{b2}\end{bmatrix},$$

$$\mathbf{C_f}=\mathbf{C_f^d}+\mathbf{C_f^b}-j\Omega\mathbf{G}^d,\quad \mathbf{C_r}=j2\Omega\mathbf{M_r},$$

$$\mathbf{K_f^s}=\begin{bmatrix} k_r & -jk_{r\theta} & -l_2k_r+k_{r\theta}/L & -l_1k_r-k_{r\theta}/L\\ jk_{r\theta} & k_\theta & -jl_2k_{r\theta}+jk_\theta/L & -jl_1k_{r\theta}-jk_\theta/L\\ -l_2k_r+k_{r\theta}/L & jl_2k_{r\theta}-jk_\theta/L & l_2^2k_r-2l_2k_{r\theta}/L+k_\theta/L^2+k_{b1} & l_1l_2k_r+(2l_2-1)k_{r\theta}/L-k_\theta/L^2\\ -l_1k_r-k_{r\theta}/L & jl_1k_{r\theta}+jk_\theta/L & l_1l_2k_r+(2l_2-1)k_{r\theta}/L-k_\theta/L^2 & l_1^2k_r+2l_1k_{r\theta}/L+k_\theta/L^2+k_{b2}\end{bmatrix}$$

$$\mathbf{K_r}=\begin{bmatrix} \Delta k_r & j\Delta k_{r\theta} & -l_2\Delta k_r+\Delta k_{r\theta}/L & -l_1\Delta k_r-\Delta k_{r\theta}/L\\ j\Delta k_{r\theta} & \Delta k_\theta & -jl_2\Delta k_{r\theta}-j\Delta k_\theta/L & -jl_1\Delta k_{r\theta}+j\Delta k_\theta/L\\ -l_2\Delta k_r+\Delta k_{r\theta}/L & -jl_2\Delta k_{r\theta}-j\Delta k_\theta/L & l_2^2\Delta k_r-2l_2\Delta k_{r\theta}/L-\Delta k_\theta/L^2 & l_1l_2\Delta k_r+(2l_2-1)\Delta k_{r\theta}/L+\Delta k_\theta/L^2\\ -l_1\Delta k_r-\Delta k_{r\theta}/L & -jl_1\Delta k_{r\theta}+j\Delta k_\theta/L & l_1l_2\Delta k_r+(2l_2-1)\Delta k_{r\theta}/L+\Delta k_\theta/L^2 & l_1^2\Delta k_r+2l_1\Delta k_{r\theta}/L-\Delta k_\theta/L^2\end{bmatrix},$$

$$\mathbf{K_f}=\mathbf{K_f^s}-j\Omega\mathbf{C_f^d},\quad L=L_1+L_2,\ l_1=L_1/L,\ l_2=L_2/L, \tag{A1}$$

where the physical parameters are

$$k_r=\left(k_\xi+k_\eta\right)/2,\ k_\theta=\left(k_{\theta_\xi}+k_{\theta_\eta}\right)/2,$$

$$k_{r\theta}=\left(k_{\xi\theta_\eta}+k_{\eta\theta_\xi}\right)/2.$$

Here, J_p and J are the polar and diametrical mass

moments of inertia of the disk; c_r and c_θ (k_r and k_θ) are the shaft linear and angular internal dampings (stiffnesses); $k_{r\theta}$ is the coupled linear and angular stiffness of the shaft; c_b and k_b are the bearing damping and stiffness; y_d and z_d (θ_y and θ_z) denote the linear (angular) displacements of the disk; y_1 and z_1 (y_2 and z_2) denote the linear displacements of bearing #1 (#2), in the y-z directions; f_{y_d} and f_{z_d} ($f_{\theta y}$ and $f_{\theta z}$) are the forces (moments) acting on the disk in the y-z directions; ΔJ, Δk_r, Δk_θ, $\Delta k_{r\theta}$, Δc_r, Δc_θ, $\Delta c_{b1,2}$ and $\Delta k_{b1,2}$ are their deviatoric values. The shaft stiffnesses can be obtained from the structural mechanics as (Kramer, 1993)

$$
\begin{aligned}
k_\xi &= 3\left(EI_{\xi_1}/L_1^3 + EI_{\xi_2}/L_2^3\right),\\
k_\eta &= 3E\left(I_{\eta_1}/L_1^3 + I_{\eta_2}/L_2^3\right),\\
k_{\xi\theta_\eta} &= 3E\left(-I_{\xi_1}/L_1^2 + I_{\xi_2}/L_2^2\right),\\
k_{\eta\theta_\xi} &= 3E\left(-I_{\eta_1}/L_1^2 + I_{\eta_2}/L_2^2\right),\\
k_{\theta_\xi\theta_\xi} &= 3E\left(I_{\xi_1}/L_1 + I_{\xi_2}/L_2\right),\\
k_{\theta_\eta\theta_\eta} &= 3E\left(I_{\eta_1}/L_1 + I_{\eta_2}/L_2\right),
\end{aligned}
\tag{A2}
$$

where E is the modulus of elasticity of the shaft.

Appendix B Influence coefficients

(1) Isotropic rotor system

$$\mathbf{H}_{\mathbf{g}_{;0}\mathbf{p}_{;0}}(\omega) = \mathbf{D}_{\mathrm{f};0}^{-1}, \tag{B1}$$

(2) Anisotropic rotor system

$$
\begin{aligned}
&\mathbf{H}_{\mathbf{g}_{;0}\mathbf{p}_{;0}}(\omega) = (\mathbf{D}_{\mathrm{f};0} - \mathbf{D}_{\mathrm{b};0}\bar{\mathbf{D}}_{\mathrm{f};0}^{-1}\mathbf{D}_{\mathrm{b};0})^{-1},\\
&\mathbf{H}_{\mathbf{g}_{;0}\hat{\mathbf{p}}_{;0}} = -(\bar{\mathbf{D}}_{\mathrm{f};0} - \bar{\mathbf{D}}_{\mathrm{b};0}\mathbf{D}_{\mathrm{f};0}^{-1}\mathbf{D}_{\mathrm{b};0})^{-1}\bar{\mathbf{D}}_{\mathrm{b};0}\mathbf{D}_{\mathrm{f};0}^{-1},
\end{aligned}
\tag{B2}
$$

(3) Asymmetric rotor system

$$
\begin{aligned}
&\mathbf{H}_{\mathbf{g}_{;0}\mathbf{p}_{;0}}(\omega) = (\mathbf{D}_{\mathrm{f};0} - \mathbf{D}_{\mathrm{r};0}\bar{\mathbf{D}}_{\mathrm{f};-1}^{-1}\bar{\mathbf{D}}_{\mathrm{r};-1})^{-1},\\
&\mathbf{H}_{\mathbf{g}_{;0}\hat{\mathbf{p}}_{;-1}}(\omega) = -(\bar{\mathbf{D}}_{\mathrm{f};-1} - \bar{\mathbf{D}}_{\mathrm{r};-1}\mathbf{D}_{\mathrm{f};0}^{-1}\mathbf{D}_{\mathrm{r};0})^{-1}\bar{\mathbf{D}}_{\mathrm{r};-1}\mathbf{D}_{\mathrm{f};0}^{-1},
\end{aligned}
\tag{B3}
$$

(4) General rotor system (6 N reduced order Hill's matrix)

$$
\begin{aligned}
&\mathbf{H}_{\mathbf{g}_{;0}\mathbf{p}_{;0}}(\omega) = -\mathbf{h}_3^{-1}\mathbf{h}_2,\\
&\mathbf{H}_{\mathbf{g}_{;0}\hat{\mathbf{p}}_{;0}}(\omega) = -\bar{\mathbf{D}}_{\mathrm{f};0}^{-1}\\
&\qquad\left(\bar{\mathbf{D}}_{\mathrm{r};1}\mathbf{h}_5^{-1}\mathbf{h}_4^{-1}\mathbf{D}_{\mathrm{f};-1}^{-1}\mathbf{D}_{\mathrm{r};0}\bar{\mathbf{D}}_{\mathrm{f};0}^{-1} + \mathbf{I}\right)\\
&\qquad\bar{\mathbf{D}}_{\mathrm{b};0}\mathbf{H}_{\mathbf{g}_{;0}\mathbf{p}_{;0}},\\
&\mathbf{H}_{\mathbf{g}_{;0}\hat{\mathbf{p}}_{;-1}}(\omega) = \left(\bar{\mathbf{D}}_{\mathrm{f};-1}^{-1}\bar{\mathbf{D}}_{\mathrm{b};-1}\mathbf{D}_{\mathrm{f};1}^{-1}\mathbf{D}_{\mathrm{b};1} - \mathbf{I}\right)^{-1}\\
&\qquad\bar{\mathbf{D}}_{\mathrm{f};-1}^{-1}\bar{\mathbf{D}}_{\mathrm{r};0}\mathbf{H}_{\mathbf{g}_{;0}\mathbf{p}_{;0}},\\
&\mathbf{H}_{\mathbf{g}_{;0}\mathbf{p}_{;-1}}(\omega) = \mathbf{D}_{\mathrm{f};1}^{-1}\mathbf{D}_{\mathrm{b};1}\left(\bar{\mathbf{D}}_{\mathrm{f};-1}^{-1}\bar{\mathbf{D}}_{\mathrm{b};-1}\mathbf{D}_{\mathrm{f};1}^{-1}\mathbf{D}_{\mathrm{b};1} - \mathbf{I}\right)^{-1}\\
&\qquad\bar{\mathbf{D}}_{\mathrm{f};-1}^{-1}\bar{\mathbf{D}}_{\mathrm{r};0}\mathbf{H}_{\mathbf{g}_{;0}\mathbf{p}_{;0}},\\
&\mathbf{H}_{\mathbf{g}_{;0}\mathbf{p}_{;1}}(\omega) = \mathbf{h}_5^{-1}\mathbf{h}_4^{-1}\mathbf{D}_{\mathrm{f};-1}^{-1}\mathbf{D}_{\mathrm{r};0}\bar{\mathbf{D}}_{\mathrm{f};0}^{-1}\bar{\mathbf{D}}_{\mathrm{b};0}\mathbf{H}_{\mathbf{g}_{;0}\mathbf{p}_{;0}},\\
&\mathbf{H}_{\mathbf{g}_{;0}\hat{\mathbf{p}}_{;1}}(\omega) = -\bar{\mathbf{D}}_{\mathrm{f};1}^{-1}\bar{\mathbf{D}}_{\mathrm{b};1}\mathbf{h}_5^{-1}\mathbf{h}_4^{-1}\mathbf{D}_{\mathrm{f};-1}^{-1}\\
&\qquad\mathbf{D}_{\mathrm{r};0}\bar{\mathbf{D}}_{\mathrm{f};0}^{-1}\bar{\mathbf{D}}_{\mathrm{b};0}\mathbf{H}_{\mathbf{g}_{;0}\mathbf{p}_{;0}},
\end{aligned}
\tag{B4}
$$

where $\mathbf{h}_1$, $\mathbf{h}_2$, $\mathbf{h}_3$, $\mathbf{h}_4$ and $\mathbf{h}_5$ are

$$
\begin{aligned}
&\mathbf{h}_1 = \bar{\mathbf{D}}_{\mathrm{b};0}\mathbf{D}_{\mathrm{f};0}^{-1}\mathbf{D}_{\mathrm{b};0} + \bar{\mathbf{D}}_{\mathrm{r};0}(\mathbf{D}_{\mathrm{f};-1} - \mathbf{D}_{\mathrm{b};-1}\bar{\mathbf{D}}_{\mathrm{f};1}^{-1}\bar{\mathbf{D}}_{\mathrm{b};1})^{-1}\\
&\qquad\mathbf{D}_{\mathrm{r};-1} - \bar{\mathbf{D}}_{\mathrm{b};0},\\
&\mathbf{h}_2 = \mathbf{I} - \mathbf{D}_{\mathrm{b};0}\mathbf{h}_1^{-1}\bar{\mathbf{D}}_{\mathrm{b};0}\mathbf{D}_{\mathrm{f};0}^{-1},\\
&\mathbf{h}_3 = \mathbf{h}_2\mathbf{D}_{\mathrm{r};0}(\bar{\mathbf{D}}_{\mathrm{f};-1} - \bar{\mathbf{D}}_{\mathrm{b};-1}\mathbf{D}_{\mathrm{f};1}^{-1}\mathbf{D}_{\mathrm{b};1})^{-1}\bar{\mathbf{D}}_{\mathrm{r};-1} - \mathbf{D}_{\mathrm{f};0},\\
&\mathbf{h}_4 = \mathbf{D}_{\mathrm{f};-1} - \mathbf{D}_{\mathrm{r};0}\bar{\mathbf{D}}_{\mathrm{f};0}^{-1}\mathbf{D}_{\mathrm{r};1},\\
&\mathbf{h}_5 = \mathbf{I} - \bar{\mathbf{D}}_{\mathrm{f};1}^{-1}\bar{\mathbf{D}}_{\mathrm{b};1}\mathbf{h}_4^{-1}\mathbf{D}_{\mathrm{b};-1}.
\end{aligned}
$$